

## Characteristics of Solid Hold Up and Circulation Rate in the CFB Reactor with 3-Loops

Jong-Min Lee<sup>†</sup>, Jae-Sung Kim and Jong-Jin Kim

Advanced Power Generation & Combustion Group, Power Generation Lab.,  
Korea Electric Power Research Institute, KEPCO, Daejeon 305-380, Korea  
(Received 5 March 2001 • accepted 2 July 2001)

**Abstract**—The effects of the  $U_o$ , PA/[PA+SA] ratio, total solid inventory and fluidizing velocity of loopseal on the axial solid holdup and the solid circulation rate have been determined with different particle sizes (174, 199, 281, 377  $\mu\text{m}$ ) and particle types (silica sand: narrow PSD, coal ash: wide PSD) in a CFB reactor with 3-loops. A simple model for solid hold-up based on the previous works was in agreement with the experimental data. With increasing  $U_o$ ,  $G_s$  increased exponentially, and in the center-loop,  $G_s$  was 1.5 times larger than that found in the other side-loops. As the PA/[PA+SA] ratio increased, and as SA injection port was placed at a lower part in the riser, the axial solid holdup and  $G_s$  increased. With increasing fluidizing velocity of loopseal to about  $1.5u_{mf}$ ,  $G_s$  somewhat increased, but above the gas velocity of  $1.5u_{mf}$ , the loopseal lost the ability of the control of  $G_s$ . The following correlation for the solid circulation rate in the CFB was developed with good accuracy;  $G_s = \phi_{3\text{ys}} [\text{PA}/\text{TA}]^{2.6} [\text{H}_r/\text{H}_t]^{0.5} [\text{Ar}]^{-1.888} [\text{Fr}]^{2.06} [\text{KU}_o/U_i]^{-3.45}$ .

Key words: CFB, 3-Loops, Axial Solid Hold-Up, Solid Circulation Rate

### INTRODUCTION

The circulating fluidized bed (CFB) has been successfully used in the petroleum refining industry for the catalytic cracking of crude oil since the early 40's. Its industrial use for noncatalytic reactions started with the Lurgi CFB calciner around 1970, and during the 1980's CFB's found wide application for combustion [Grace et al., 1996]. CFB combustion technology is now economically so important that about 240 CFB combustion units (>50 MWth) with a total power of 36,000 MWth are in operation. One of these CFB units is the Tonghae CFB power plant with a total power for 400 MWe (200 MWe  $\times$  2 unit) in Korea. It has been under commercial operation since 1998, where Korean anthracite is used as fuel [Lee and Kim, 1999]. The Tonghae CFB boiler consists of a rectangular furnace, three cyclones, loopseals and fluidized bed heat exchangers (FBHEs) and a fluidized bed ash cooler (FBAC). Unlike the existing CFB units, the furnace of which aspect ratio is more than 2 : 1 has three loops for circulation of solid particles. In the furnace, coal ash is only used as bed material due to much ash in coal fed. Therefore, the characteristics of the gas and solid flow are expected to be somewhat different.

On the other hand, knowledge of the flow pattern of gas and particles in the CFB is important for a description of heat transfer and temperature profile and for mapping of the distribution of unburned fuel particles in the bed [Choi et al., 1995]. Additionally, the solid circulation rate is an important parameter to affect the flow pattern of gas and particles and to design the cyclone, downcomer and non-mechanical valve. Detailed studies of the flow pattern in CFBs have been extensively investigated during recent years. However, most works were carried out in rather small-scale CFBs and some industrial studies were tedious and costly. Pressure drop measurements,

on the other hand, are a relatively simple way to determine the overall vertical profile of the cross-sectional average solids concentra-

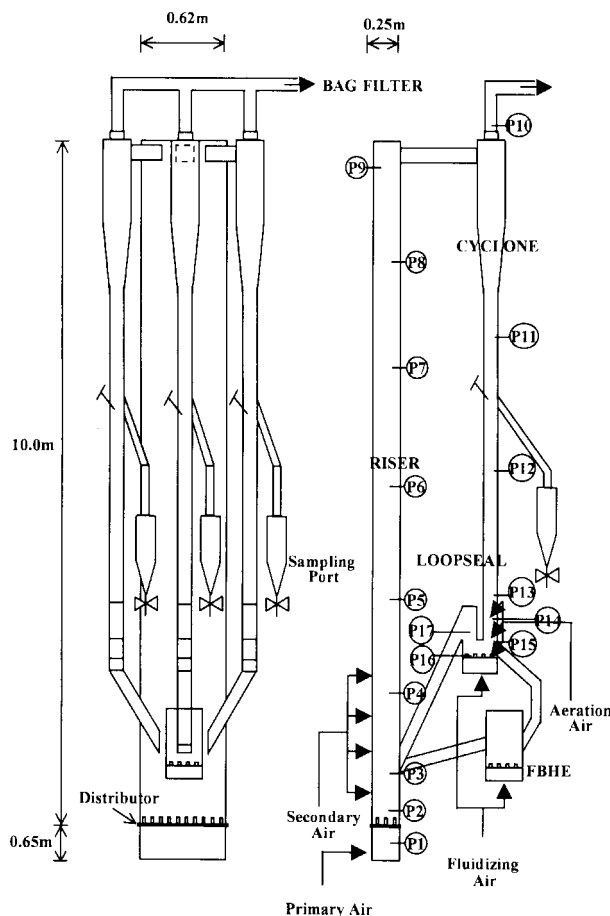


Fig. 1. Schematic diagram of the CFB reactor.

<sup>†</sup>To whom correspondence should be addressed.  
E-mail: jmllee@kepri.re.kr

tion [Choi et al., 1990; Kim et al., 1999].

Therefore, the aim of the present work is to study the overall flow pattern and to predict the solid circulation rate by means of the pressure drop measurements with various operation conditions in a cold CFB reactor that was similarly designed to the Tonghae CFB reactor. Of special interest is the character of the transport zone of the CFB in which information of the particle size distribution and the solid circulation rate emerges.

**EXPERIMENT**

Experiments were carried out in a cold CFB reactor having 3-cyclones as shown in Fig. 1. It consists of a main CFB reactor, a system of air supplier and controller, devices of pressure measurement, and a bagfilter system for collecting fine particles. The main CFB reactor is composed of a rectangular riser [0.25 m (L)×0.62 m (W)×10.0 m (H)], 3-cyclones [0.365 m (I.D.)×1.46 m (H)] and loopseals [0.1 m (I.D.)] and a FBHE [0.3 m (L)×0.3 m (W)×0.5 m (H)], where the system geometry was designed like the Tonghae CFB boiler. The secondary air was introduced through 4 nozzles of each sidewall at interval of 0.5 m above the primary air distributor. Air for fluidizing particles of loopseals was introduced through a bubble cap distributor and through the aeration nozzles mounted with the dipleg of the loopseal. The pressures were registered in 33 pressure taps mounted with the surface of one of the sidewalls at different heights. Solid circulation rates were calculated by weight measurement of particles bypassing from downcomers to sampling ports for constant time.

Three silica sands with average particle diameters of 199, 288 and 377 μm, and a coal ash with average particle diameter of 174 μm were used as bed materials. The coal ash has wider size distribution than that of silica sands, as shown in Fig. 2. The properties of the particles are summarized in Table 1.

The gas velocity in the riser was determined to be 1.4-4.4 m/s, which gives a similar flow regime of the Tonghae CFB furnace [Lee

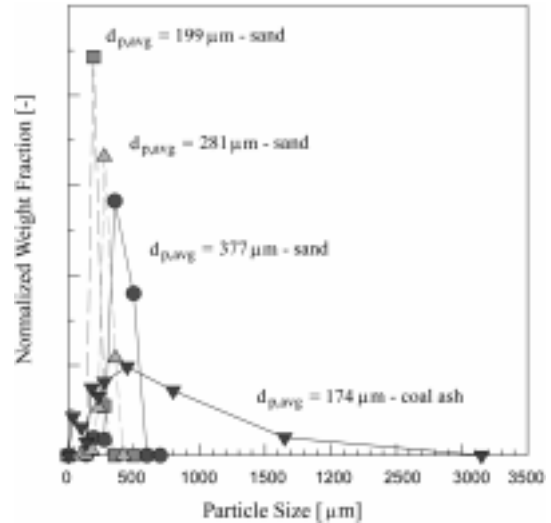


**Fig. 2. Particle size distribution of silica sand and coal ash.**

**Table 1. Properties of the solid particles used as bed material**

	Coal ash		Silica sand	
$d_{p,avg}$ (μm)	177	199	281	377
$\rho_s$ (kg/m <sup>3</sup> )	2300	2800	2800	2800
$U_{mf}$ [Wen and Yu, 1966] (m/s)	0.023	0.036	0.071	0.125
$U_c$ [Kunii and Levenspiel, 1991] (m/s)	1.004	1.621	2.393	3.177

et al., 2000]. The axial solid holdup in the riser was obtained by measurement of pressure differences between the pressure taps.

**RESULT AND DISCUSSION**

Fig. 3 shows the axial solid holdup in the riser for the 377 μm

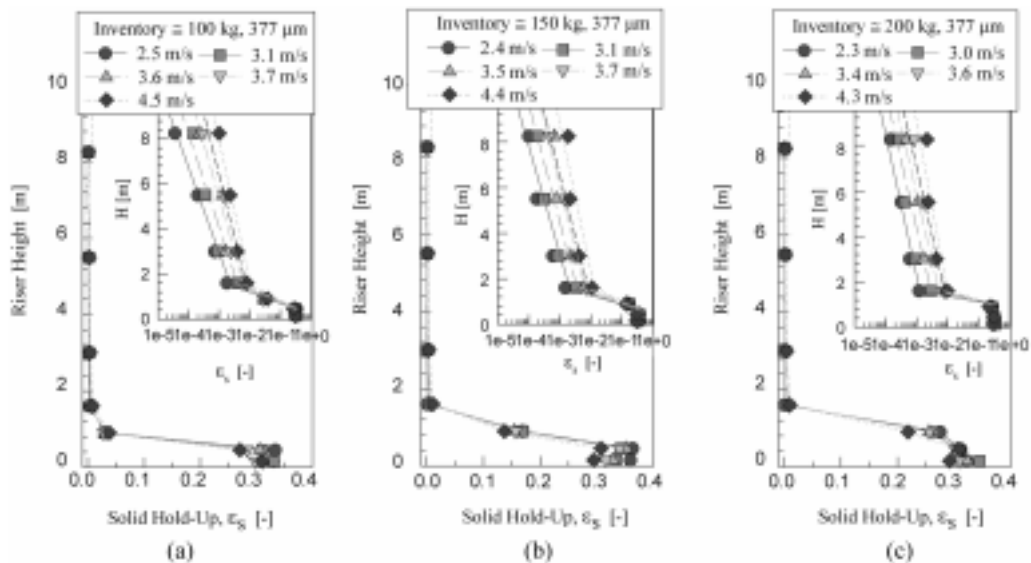


**Fig. 3. Axial solid hold up with riser velocity,  $U_r$ .**  
 (a) inventory=100 kg, (b) inventory=150 kg, (c) inventory=200 kg

silica sand with  $U_o$  (2.3-4.5 m/s) and solid inventory (100-200 kg). The axial solid holdup was calculated from pressure drop by using the following equation.

$$\frac{\Delta P}{L} = (1 - \epsilon_s)(\rho_s - \rho_g) \frac{g}{g_c} \quad (1)$$

Three zones could be identified in the axial solid hold up in all cases in spite of the different solid circulation rate and  $U_o$ , and especially,  $U_o$  not exceeding the terminal velocity: a dense region with a constant axial solid holdup close to the gas distributor, a splash region where the gradient changes considerably and a transport region from about 1.5 meters height all the way up to the riser exit with a low change of axial solid holdup. The solid holdup in the dense region was about 0.3-0.35, which was similar to that of a bubbling bed, and did not change appreciably with  $U_o$  because  $U_o$  was relatively lower and just kept the flow regime to be turbulent or in initial state of fast fluidization. The dense bed height decreased with  $U_o$  and increased with solid inventory. In the splash region, the axial solid holdup changed considerably to increase and its slope increased, as  $U_o$  increased. In the transport region the axial solid holdup was very low ( $10^{-5}$ - $10^{-3}$ ) and its slope also increased with  $U_o$ . Similar results were obtained when varying the particle size of silica sand and the particle type to coal ash. It is possible to describe the axial solids holdup based on empirical data and knowledge of the local flow pattern. Johnsson and Lecker [1995] proposed simple model equations based on the previous studies [Bolton and Davidson, 1988; Kunii and Levenspiel, 1990; Zhang and Johnsson, 1991; Harris et al, 1993; Zhang et al., 1993]. The model equations are expressed as follows,

$$\epsilon_s = \epsilon_{sd} \quad \text{for } h < H_d \quad (2)$$

$$\epsilon_s = (\epsilon_d - \epsilon_{t,x})e^{-a(h-H_d)} + \epsilon_{ext}e^{K(U_o/U_t - h)} \quad \text{for } H_d < h < H_{ext} \quad (3)$$

$$\text{where, } \epsilon_{t,x} = \epsilon_{ext}e^{K(U_o/U_t - H_d)} \quad (4)$$

Decay constant  $a$  and  $K$  for the silica sand particles could be obtained from the slope of the axial solid holdup in Fig. 3, where the

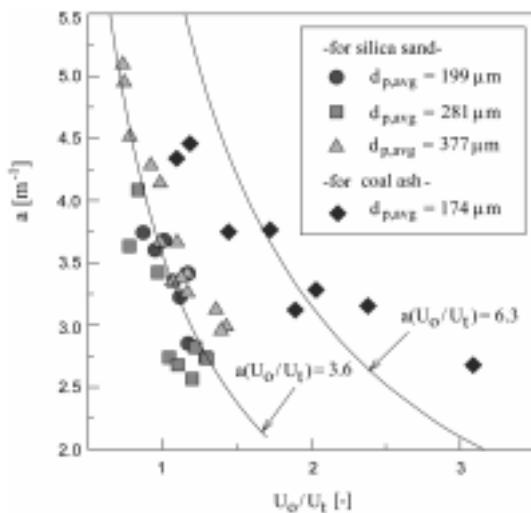


Fig. 4. Decay constant  $a$  vs.  $U_o/U_t$  for silica sand and coal ash particles.

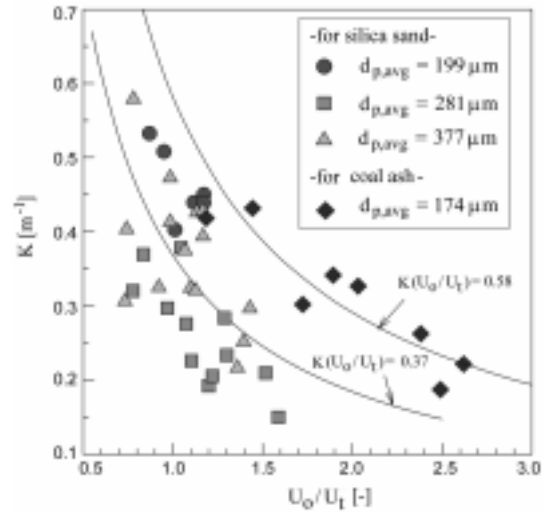


Fig. 5. Decay constant  $K$  vs.  $U_o/U_t$  for silica sand and coal ash particles.

slope in the splash region and in the transport region represented decay constants  $a$  and  $K$ , respectively. The decay constants  $a$  and  $K$  were plotted vs. gas velocity related to terminal velocity in Fig. 4 and Fig. 5, respectively. Fig. 4 showed that the equation of  $aU_o = \text{constant}$  proposed by Kunii and Levenspiel [1990], where the constant changes with different particle size, could be rewritten as  $aU_o/U_t = \text{constant}$ . Fig. 5 shows that the equation of  $K(U_o - U_t) = \text{constant}$  proposed by Johnsson and Leckner [1995], where the equation cannot be used if  $U_o$  is less than  $U_t$ , could be also rewritten as  $KU_o/U_t = \text{constant}$ . This means that solid particles can be entrained even if  $U_o$  is less than  $U_t$  when the average particle size and its terminal velocity are adopted to analyze the overall flow pattern of the furnace. This also shows that the net solid transfer coefficient  $\kappa$ , which is derived from the equation of  $K = 4\kappa/[D_c(U_o - U_t)]$  proposed by Zhang and Johnsson [1991] in the transport region, cannot be independent of  $U_o$  though Johnsson and Leckner proposed that  $K(U_o - U_t)$  was constant and  $\kappa$  was independent of  $U_o$ .

The decay constants  $a$  and  $K$  of silica sand and coal ash particles could be expressed as follows.

For silica sand,

$$aU_o/U_t = 3.6 \quad (5)$$

$$KU_o/U_t = 0.37 \quad (6)$$

For coal ash,

$$aU_o/U_t = 6.30 \quad (7)$$

$$KU_o/U_t = 0.58 \quad (8)$$

The constants  $a$  and  $K$  for the coal ash particles are larger than those of silica sand particles. This may result from segregation of particles in the transport region due to wide size distribution.

The solid circulation rate,  $G_s$  with particle size and  $U_o$  related  $U_o/U_t$  for silica sand was plotted logarithmically in Fig. 6.  $G_s$  increased linearly with  $U_o/U_t$ , and may be independent of particle size. Solid circulation rate in the center loop was 1.5 times larger than that of the other side loops and could be written as

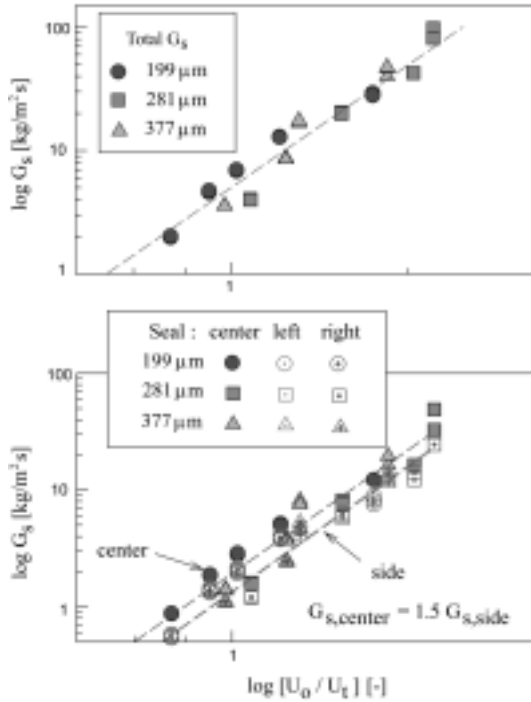


Fig. 6. Solid circulation rate,  $G_s$ , vs.  $U_o/U_t$  with particle size of silica sand.

$$G_{s,center} = 1.5 G_{s,side} \quad (9)$$

The solid circulation rate for coal ash showed a similar result, but was much lower than that for silica sand due to wide size distribution of coal ash.

The axial solid holdup and its slope in the splash region and transport region increased with increasing the ratio of primary to total air flow rate from 0.66 to 1.0. With increasing solid inventory from 100 kg to 200 kg, the solid holdup increased but its slope did not change appreciably in these regions. The solid circulation rate also increased linearly with increasing the air ratio and solid inventory, whereas it increased exponentially with increasing the riser velocity, as shown in Fig. 7(a) and (b). On the other hand, the axial solid holdup and the solid circulation rate were found to be increased as the secondary air was introduced at lower injection port. From these results, it was found that the solid holdup and circulation rate increased linearly with increasing the contact frequency between particles and gas.

With increasing fluidizing velocity of the loopseal to about  $1.5U_{mf}$ , solid circulation rate,  $G_s$ , somewhat increased, but above the gas velocity of  $1.5U_{mf}$ ,  $G_s$  did not change appreciably. As fluidizing velocity in the loopseal increased,  $G_s$  was likely to decrease because the fluidizing air of loopseal interfered with the downflow of the solid particles in the downcomer [Kim et al., 1999]. This is why the solid inventory in the riser changes in conjunction with the solid inventory in the loopseal though the total solid inventory in the CFB is constant. The solid inventory in the loopseal changes due to non-uniform fluidization and non-uniform feeding of the solid particles to the riser, and consequently that causes a change in the solid inventory of the riser when the fluidizing velocity in the loopseal is relatively low. Therefore, the contact chance between solid parti-

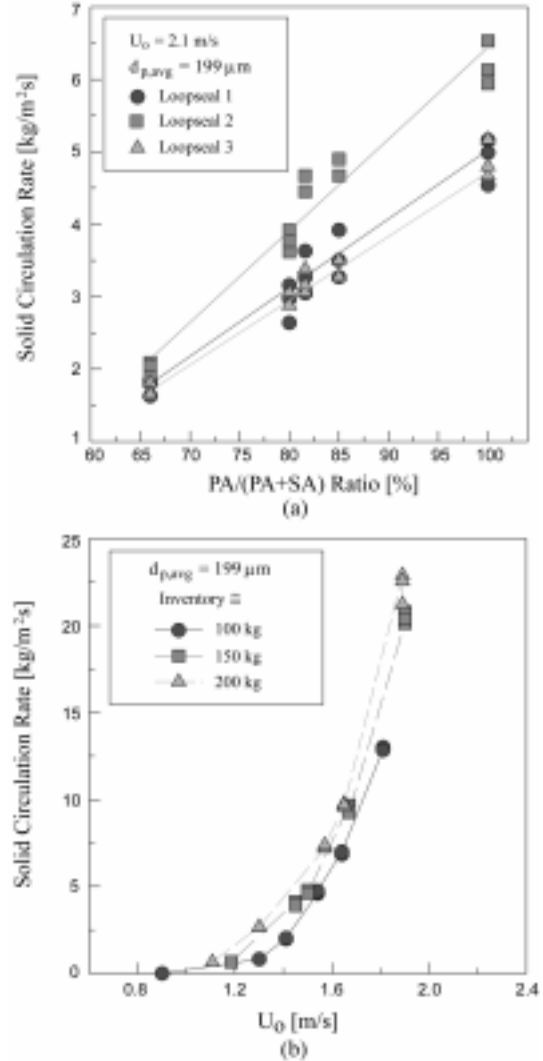


Fig. 7. Effects of (a) PA/[PA+SA] ratio and (b) solid inventory on the solid circulation rate.

cles and fluidizing gas in the riser may be reduced and  $G_s$  decreases when the fluidizing gas in the loopseal is not sufficient. Similar results were obtained when the aeration air (grease air) at the dipleg was injected to the loopseal.

To predict the solid circulation rate with operation variables in this CFB reactor, the following correlation was developed:

$$G_s = \phi_{sys} [PA/TA]^{2.6} [H/H_7]^{0.5} [Ar]^{-1.88} [Fr]^{2.06} [KU_o/U_r]^{-3.45} \quad (10)$$

$$\text{Correlation coefficient} = 0.96 \text{ and regression coefficient} \\ = 0.93, \phi_{sys} = 2.0$$

In this correlation, the character of the solid holdup in the transport was introduced as the term of  $[KU_o/U_r]$  that could represent the information of the particle size distribution. This correlation based on the operating parameters and pressure drop measurements is relatively simple to predict the solid circulation rate. The calculated result from the correlation for the different particles investigated and the previous work is shown in Fig. 8 with experimental results. The correlation for the solid circulation rate is in agreement with the experimental data with good accuracy.

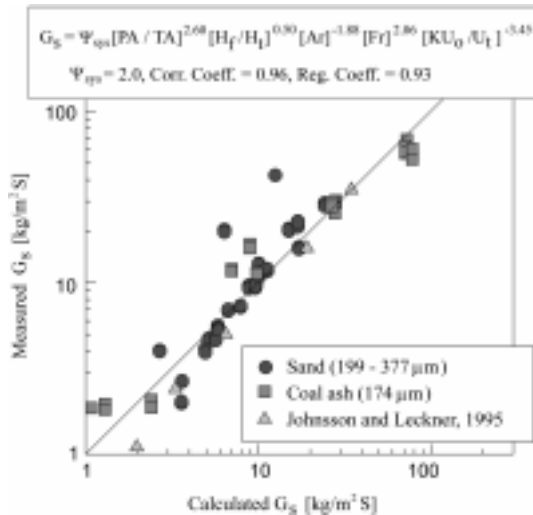


Fig. 8. Correlation for the solid circulation rate.

### CONCLUSION

Hydrodynamic characteristics in a cold CFB with 3-cyclones, which was designed by the analogy with the Tonghae CFB, has been determined with operating parameters such as  $U_o$ , PA/[PA+SA] ratio, total solid inventory and fluidizing velocity of loopseal for the different particle sizes and types. Axial solid holdup distribution could be explained by using decay constants  $a$  and  $K$  which were obtained from splash and dilute phases, respectively. The constants obtained from the equations of  $aU_o/U_t$  and  $KU_o/U_t$  for the wide size distribution of the coal ash were higher than those of silica sand, whereas the solid holdup and the solid circulation rate were lower. With increasing  $U_o$ , the solid circulation rate increased exponentially and in the center-loop it was 1.5 times higher value than that found in the other side-loops. The simple correlation for the solid circulation rate with operation variables in the CFB was developed and seemed to be with good accuracy.

### NOMENCLATURE

$a, K$  : decay constant [ $m^{-1}$ ]  
 $Ar, Fr$  : Archimedes number and Froude number, respectively [-]  
 $G_s$  : solid circulation rate [ $kg/m^2 s$ ]

$h, H_d, H_{exit}, H_f, H_t$  : height, for bottom bed, exit, fixed bed, total bed, respectively [m]  
 $k$  : net solids transfer coefficient [m/s]  
 $PA, TA$  : primary air flow rate and total air flow rate, respectively [ $kg/s$ ]  
 $U_o, U_{mf}, U_t$  : superficial gas velocity, minimum fluidizing velocity and terminal velocity [m/s]  
 $\epsilon_s, \epsilon_{sd}, \epsilon_{exit}$  : solid hold up, for dense region, exit, respectively [-]  
 $\phi_{sys}$  : system constant that varies according to system [-]  
 $\rho_s, \rho_g$  : density of solid and density of gas, respectively [ $kg/m^3$ ]

### REFERENCES

- Choi, J. H., Cho, Park, J. H., Choung, W. M., Kang, Y. and Kim, S. D., "Hydrodynamic Characteristics of Fine Particles in the Riser and Standpipe of a Circulating Fluidized Bed," *Korean J. Chem. Eng.*, **12**, 141 (1995).  
 Choi, J. H., Yi, C. K. and Son, J. E., "Axial Voidage Profile in a Cold Model Circulating Fluidized Bed," *Korean J. Chem. Eng.*, **7**, 306 (1990).  
 Grace, J. R., Avidan, A. A. and Knowlton, T. M., "Circulating Fluidized Beds," Blackie A&P, Blackie Academic & Professional, London, UK (1997).  
 Johnson, F. and Leckner, B., "Vertical Distribution of Solids in a CFB Furnace," 13<sup>th</sup> Int. Conf. on FBC, Florida, USA, 671 (1995).  
 Johnson, F., Andersson, S. and Leckner, B., "Expansion of a Freely Bubbling Fluidized Bed," *Powder Technology*, **68**, 117 (1991).  
 Kim, S. W., Namkung, W. and Kim, S. D., "Solid Flow Characteristics in Loop Seal of a Circulating Fluidized Bed," *Korean J. Chem. Eng.*, **16**, 82 (1999).  
 Kunii, D. and Levenspiel, O., "Fluidization Engineering," Butterworths Heinemann, USA (1991).  
 Lee, J. M. and Kim, J. S., "Simulation of the 200MWe Tonghae Thermal Power Plant CFB Combustor by using IEA-CFBC Model," *Korean J. Chem. Eng.*, **16**, 640 (1999).  
 Lee, J. M., Kim, J. S., Kim, S. M., Kim, J. J. and Song, K. K., "Characteristics of Axial Solid Hold-up Distribution in a CFB Riser with 3-Loops," *Energy Engg. J.*, **9**, 348 (2000).  
 Wen, C. Y. and Yu, Y. H., "A Generation Method for Predicting the Minimum Fluidization Velocity," *AIChE J.*, **12**, 610 (1966).  
 Zhang, W. and Johnson, F., "Fluid Dynamic Boundary Layers in Circulating Fluidized Bed Boiler," Report A91-193, Dept. of Energy Conversion, Chalmers Univ., Sweden (1991).